Brazilian Journal of Physics (2024) 54:21
https://doi.org/10.1007/s13538-023-01401-x

NUCLEAR PHYSICS;

Neutron Single-Particle States in ^{101}Sn by Polynomial Fits and Shell Model Calculations for Light Sn Isotopes

Abderrahmane Yakhelef[1,2] · **Serkan Akkoyun**[3]

Received: 8 July 2023 / Accepted: 21 November 2023 / Published online: 30 November 2023

Abstract
The neutron single-particle energies (SPEs) in ^{101}Sn are one of the main ingredients needed in nuclear studies in the region around the doubly magic ^{100}Sn nucleus. Due to the lack of experimental data on ^{101}Sn spectrum, the determination of SPEs needed for nuclear structure, reaction, and astrophysics studies is a real challenge. This paper discusses the derivation of the relative SPEs outside the doubly magic ^{100}Sn nucleus using a systematic method. We performed 2nd order polynomial fits for each set of experimental data corresponding to the single-particle states $d_{3/2}$, $h_{11/2}$, and $s_{1/2}$ in light odd tin isotopes. By obtaining the single-particle spectrum of ^{101}Sn, neutron SPEs of the model space orbitals are defined. Shell model calculations for even and odd $^{102-107}$Sn isotopes are carried out usin g the new interactions, fit1 and fit2. The energy spectra obtained from fit1 and fit2 are presented in comparison with the available experimental data and the results from the other interactions (well-known interaction sn100pn, pc1 obtained by Hartree–Fock method, and set2 obtained by artificial neural network method). Among them, χ^2 test confirms that fit1, fit2, and set2 are the best to reproduce the experimental spectra of light tin isotopes.

Keywords Nuclear shell model · Single-particle energy · Sn isotope · Polynomial fit

1 Introduction

In the investigations of neutron-deficient nuclei far from the beta stability line and close to the proton dripline, ^{100}Sn isotope region is one of the unique choices. The heaviest double magic self-conjugate ^{100}Sn isotope is very attractive for many reasons such as shell evolution, change of collective properties, band termination, and magnetic rotation [1–3]. The use of high-power detector arrays and radioactive ion beams opens the opportunity to perform experimental studies in this region. By increasing the experimental excited energy information in this region, the results of the studies to be carried out with the theoretical models get closer to real experimental values. This allows more accurate approaches to be performed in nuclear structure studies and enables models to be examined with higher accuracy [4–6].

In the ^{100}Sn region, there is not enough experimental excited state energy information in the literature to obtain single-particle energy (SPE) values with great accuracy needed for the nuclear shell model calculations. Different approaches have been used in the calculations to obtain neutron SPE values due to the lack of enough experimental data for the ^{101}Sn isotope. Yakhelef and Bouldjedri [7] obtained the neutron single-particle energy values by using the experimental excited energy states of ^{107}Sn isotope which is the closest isotope to ^{101}Sn with available experimental data in the literature. Brown et al. [8] obtained neutron SPEs by using the experimental energy spectrum of the ^{131}Sn isotope. The interaction called sn100pn in that study was derived from a realistic interaction developed starting from the G-matrix of the CD Bonn nucleon-nucleon interaction. Hosaka et al. [9] derived a set of interaction named as *snet* from a bare G-matrix based on the renormalized Paris potential for $N=82$ nuclei. The SPEs of sn100pn and *snet* interactions are commonly used in the shell-model calculations performed on the ^{100}Sn region. Trivedi et al. [10] modified these neutron SPEs in the sn100pn and *snet* with the use of the value of

✉ Abderrahmane Yakhelef
a.yakhelef@univ-setif.dz

[1] Physics Department, Faculty of Sciences, Farhat Abbas Setif1 University, Setif, Algeria

[2] PRIMALab Laboratory, El-Hadj Lakhedar Batna1 University, Batna, Algeria

[3] Department of Physics, Faculty of Science, Sivas Cumhuriyet University, Sivas, Turkey

$7/2^+$ level of the ^{101}Sn isotope which is the only experimental data available for this isotope. Leander et al. [11] theoretically obtained neutron SPEs, based on Hartree–Fock with Skyrme III interaction, folded Yukawa potential and Wood-Saxon single-particle potentials, separately. Engeland et al. [12] modified the previous work mentioned by using experimental observations. Andreozzi et al. [13] resorted to the analysis of low energy spectra of isotopes with $A < 111$, since there is not enough information in the literature regarding the spectrum of the ^{101}Sn isotope. Sandulescu et al. [14] obtained neutron SPEs by fitting known one quasi-particle excitation at ^{111}Sn. Grawe et al. [15] and Schubart et al. [16] used ^{88}Sr or ^{90}Zr isotopes to theoretically obtain neutron SPEs for this region. Recently, Akkoyun and Yakhelef [17] estimated neutron single-particle energies using artificial neural networks. For this purpose, machine learning was performed by using the available experimental excited energies of Sn nuclei around ^{100}Sn. Three different interactions were obtained from 3 different sets of the experimental data. Among these, set2 interaction is the best to reproduce energy spectra of light Sn isotopes.

In the present study for the first time, we aimed to address the problem with a completely different approach from those previous studies in the literature. In the approach performed in the present study, we used 2nd order polynomial fits for each set of experimental data and made a smooth extrapolation toward the neutron drip line. Our goal is to obtain the excited energy spectrum of the ^{101}Sn isotope, which allows us to deduce neutron SPEs to be used in the nuclear shell-model calculations. Therefore, what we need to do is obtain the values of the $5/2^+$, $7/2^+$, $1/2^+$, $3/2^+$, and $11/2^-$ excited energy levels of the ^{101}Sn isotope. It has been observed that the results, we obtained from the calculations performed with the SPE values of polynomial fits, are closer to the experimental data than the other calculations, especially for low-lying states.

2 Shell Model Calculations

The nuclear shell model is one of the most suitable tools to describe the low-energy spectra of atomic nuclei [18–21]. Its main idea consists of considering the nucleus as a quantum system composed of A nucleons (Z protons and N neutrons) moving freely in a self-generated mean field. The Hamiltonian of the system can be written as in Eq. 1.

$$\mathrm{H} = \sum_{\mathrm{i}=1}^{\mathrm{A}} \mathrm{T_i} + \frac{1}{2} \sum_{\mathrm{i,j}=1}^{\mathrm{A}} \mathrm{V_{ij}} \tag{1}$$

Here, T_i is the kinetic energy of each nucleon, and V_{ij} is the interaction potential between nucleons. In order to overtake the complexity of the problem, an auxiliary one-body potential U_i is introduced due to the fact that each nucleon moves under an average potential created by all the other nucleons. The Hamiltonian can be arranged as given in Eqs. 2 and 3.

$$H = \sum_{i=1}^{A} \left[T_i + U_i\right] + \left[\frac{1}{2} \sum_{i,j=1}^{A} V_{ij} - \sum_{i,=1}^{A} U_i\right] \tag{2}$$

$$H = H_0 + H_{res} \tag{3}$$

where H_0 is the one-body Hamiltonian which describes the independent motion of the nucleons, and H_{res} represents the interaction Hamiltonian.

By using an average central potential to which a strong spin–orbit term is added, the single-particle potential generates an energy spectrum organized in shells, which explains the stable nucleon configurations corresponding to so-determined magic numbers [18]. In the shell model frame, the nucleus is composed of an inert core, made up of completely filled neutron and proton shells, plus n valence nucleons moving in a truncated model space and interacting through a model space effective interaction. The model space is spanned in general by a single major proton shell and/or a single major neutron shell above the inert core.

In any shell-model calculations, one has to start by defining a model space which is a set of active single-particle orbits outside the inert core. The basic inputs are the single-particle matrix elements (which are SPEs) and the two-body matrix elements (TBMEs). For the former, SPEs are explicitly calculated using the mean-field models or defined empirically from the available experimental data of nuclei in the direct vicinity of the doubly magic nuclei. For the latter, TBMEs are specified in terms of matrix elements of the residual interaction H_{res},$< j_1 j_2 J|H_{res}|j_3 j_4 J >$, for all possible combinations of ji orbitals in the model space. J is the total two particle's angular momentum.

In the present study, we used the sn100pn interaction obtained by Brown et al. [22] as the basis of this work. It is defined by a set of 862 TBMEs, and the SPE values have been determined using the whole excitation spectrum of ^{131}Sn. The main aim of the present work is to obtain more appropriate interaction for mass region around ^{100}Sn by using single energy spectrum of ^{101}Sn obtained by 2nd$^-$order polynomial fits.

The final step in carrying out shell-model calculations is to diagonalize the model space-effective interaction with an appropriate algorithm such as Lanczos [23]. We used one of the well-known codes, the NuShellX@MSU [24], to carry out the shell model spectroscopic calculations. It presents a development of NuShell code which contains a set of computer codes written by Brown and Rae [25].

3 Results and Discussion

3.1 Obtaining SPE Values

The experimental data of the single neutron states in light odd-Sn nuclei up to ^{131}Sn are taken from ENSDF [26] and shown in Fig. 1. We can consider ^{115}Sn as a benchmark for the evolution trend of single-particle states in odd Sn isotopes. Almost all the five states start to change their direction of variation going forward to the neutron and proton drip lines. The changes are due to the filling of each sub-shells in the model space according to neutron numbers. States that are down in the region near ^{132}Sn, $d_{3/2}$, $h_{11/2}$, and $s_{1/2}$ go up when going forward to the proton drip line near ^{100}Sn. In contrast, the other states, $d_{5/2}$ and $g_{7/2}$, which are up near ^{132}Sn go down to the ground state and the first excited state in the other side of the nuclear chart.

The lightest isotope which figures all states in its spectrum is ^{109}Sn. The state $s_{1/2}$ is still missing in the ^{107}Sn nucleus spectrum. By going down to ^{101}Sn, only the ground state and the first excited state, believed to be $d_{5/2}$ and $g_{7/2}$, respectively, are defined experimentally. The energy splitting between these two levels in this nucleus has been reported in two different measurements as 172 keV [27, 28].

The fit of the experimental data of the $g_{7/2}$ state in light odd tin isotopes, up to ^{111}Sn and up to ^{109}Sn, respectively, by 2nd-order polynomial functions gives satisfactory results. The plotted curves capture the general trend and simulate all points with very high accuracy (Fig. 2). The values of the coefficient of determination (R-squared) are high for the two fits and are equal to 0.870 and 0.975 for fit1 and fit2, respectively. Hence, experimental excitation energies of the $g_{7/2}$ state in light tin isotopes can be fitted by 2nd-order polynomial functions, especially for fit2 curves.

In order to obtain the excited states in ^{101}Sn, which are not experimentally defined, we used a 2nd-order polynomial fit for each set of data corresponding to single-particle states $d_{3/2}$, $h_{11/2}$, and $s_{1/2}$ in light odd Sn isotopes. We used two approaches based on the trend of the evolutions of states. In the first one, we took, for each one of the three states, the experimental data in odd Sn isotopes up to ^{115}Sn (fit1). In the second approach, we took only the experimental data in odd Sn isotopes up to ^{113}Sn (fit2). The choice of the former is because, as mentioned above, it is the point where the trends of the evolution of states change at ^{115}Sn. Regarding the latter, it appears that at ^{113}Sn, the curves exhibit a gradual transition toward the proton drip line. Results are represented in Fig. 2 for these two different fits. By extrapolating curves down forward to lighter isotopes, we deduce

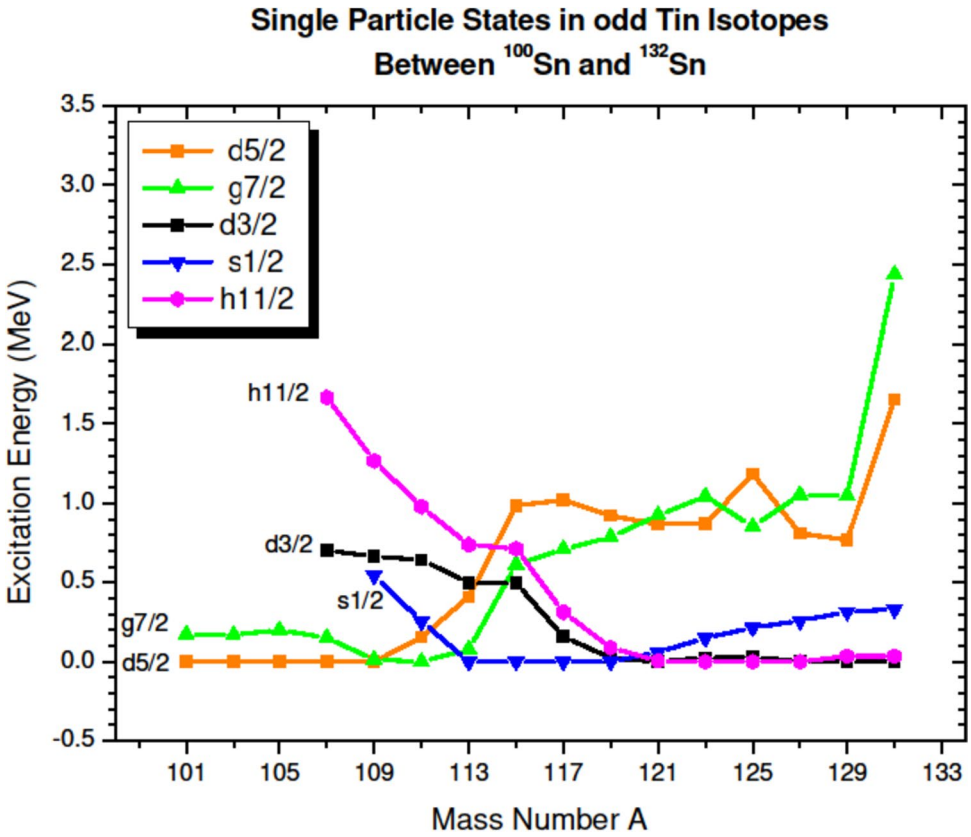

Fig. 1 Experimental neutron single-particle states in odd Sn isotopes up to ^{131}Sn. Data are from (ENSDF) Ref [26]

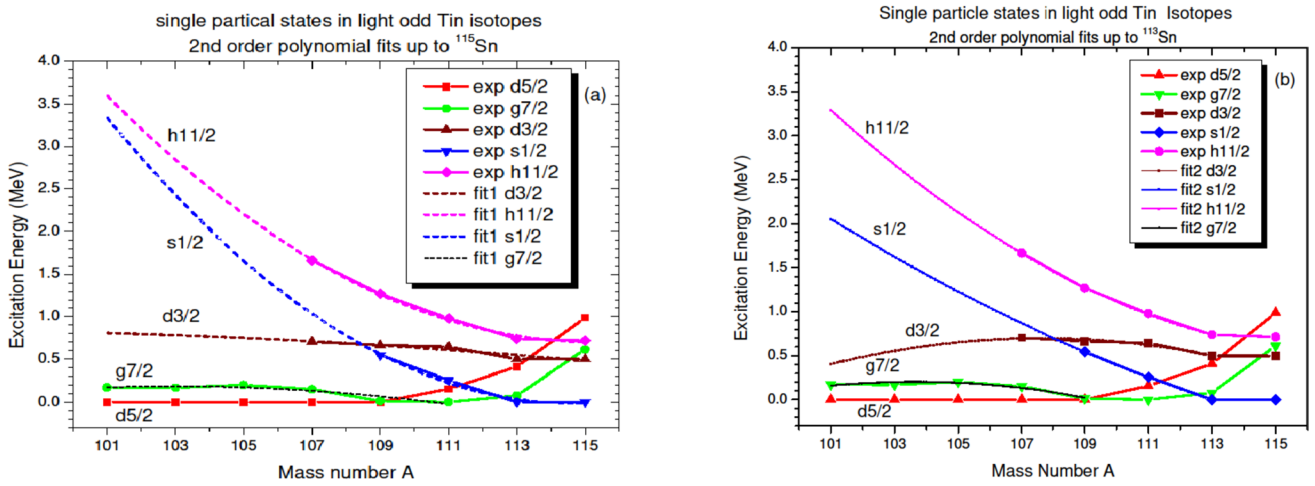

Fig. 2 Neutron single-particle states in light Sn isotopes including **a** 2nd order polynomial fit up to ^{115}Sn (fit1) and **b** 2nd order polynomial fit up to^{113}Sn (fit2)

the excitation energies of these states in ^{101}Sn. Subsequently, we can calculate the corresponding SPEs of the model space orbitals for each fit. Results are summarized in Table 1.

3.2 Single-Particle Energies by Different Methods

As mentioned before, the region around the doubly magic heavy ^{100}Sn atomic nucleus is one of the interesting topics in nuclear physics. It is very important to accurately determine the SPEs for the nuclear shell model, which is one of the commonly used tools in nuclear structure studies to be carried out in this region. The way to get the most accurate SPE values is to use the experimental spectrum of the ^{101}Sn core located just above the ^{100}Sn core. However, there is not enough information about ^{101}Sn in the literature due to the fact that the experimental studies that will enable to obtain this nucleus spectrum have not been provided at a sufficient level yet. Therefore, different approaches have been used to obtain the SPE values to be used in the nuclear shell model calculations for this region. The ^{101}Sn energy spectra obtained by these different approaches are given in Fig. 3.

Table 1 Excitation (E_{ex}) and neutron single-particle energies (SPEs) from the 2nd order polynomial fits

	Energy (MeV)				
	$d_{5/2}$	$g_{7/2}$	$d_{3/2}$	$s_{1/2}$	$h_{11/2}$
E_{ex} (fit1)	0	+0.172	+0.811	+3.347	+3.605
SPE (fit1)	−11.081	−10.909	−10.270	−7.734	−7.476
E_{ex} (fit2)	0	+0.172	+0.405	+2.054	+3.293
SPE (fit2)	−11.081	−10.909	−10.676	−9.027	−7.788
SPE of sn100pn	−10.2893	−10.6089	−8.7167	−8.6944	−8.8152

3.3 Chi-Squared (χ^2) Test

In order to evaluate the accuracy of the results obtained by the different interactions, we used the χ^2 test. It is a statistical test used to determine if there is a significant association between two categories or variables. The χ^2 tests are widely used in many scientific fields including nuclear physics to compare experimental data to predictions obtained by theoretical models [29, 30]. The formula for the χ^2 test used in our case is given in Eq. 4.

$$\chi^2 = \sum_i^n \frac{(E_{expi} - E_{thi})^2}{E_{thi}} \tag{4}$$

where n is the number of levels of the designed spectrum, and E_{expi} is the experimental energy of the ith level, while E_{thi} is its corresponding expected value predicted by shell model. For each nucleus, we calculate χ^2 for the four spectra obtained in this study and for set2 interaction obtained by artificial neural network (ANN) in our previous study [17]. The aim is to have a basis for comparison between the different methods. Results are tabulated below in Tables 2, 3, 4, 5, 6, and 7. In general, fit1, fit2, and set2 interactions are more successful to reproduce spectra of tin isotopes in this study compared to sn100pn and Hartree–Fock pc1 interactions. Seeing χ^2 values calculated for the different spectra of odd isotopes, set2 is the best to reproduce experimental spectra of ^{105}Sn and ^{107}Sn nuclei with χ^2 values of 0.026 and 0.130, respectively; while that fit1 and set2 are better for ^{103}Sn isotope with a χ^2 value of 0.031 and 0.030, respectively. χ^2 test for even isotopes gives similar results where

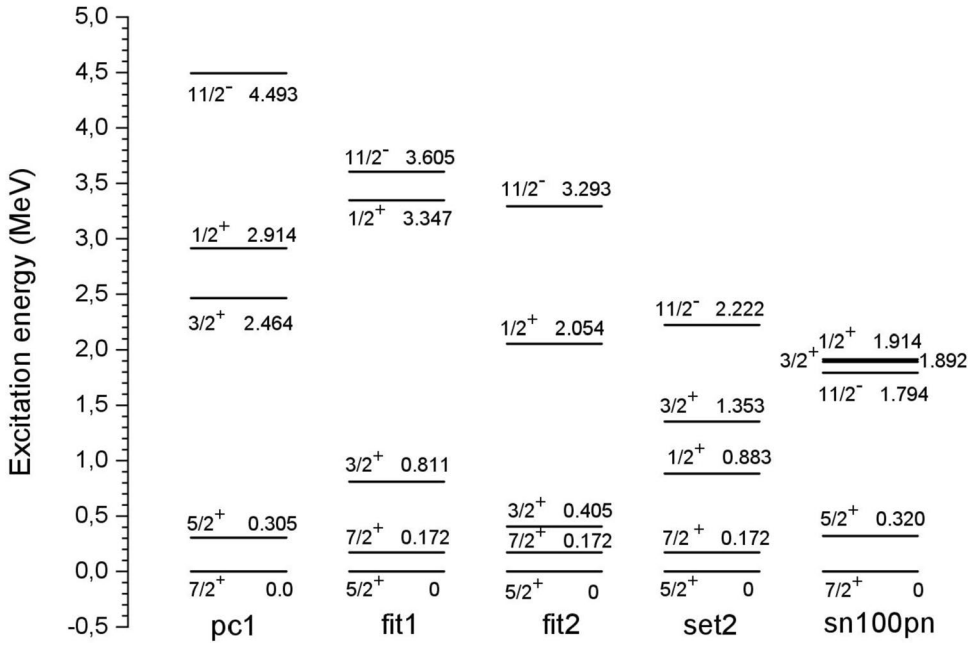

Fig. 3 Single-particle energy spectra of ^{101}Sn obtained by pc1 (Hartree–Fock method), fit1 and fit2 (2nd order polynomial fits), set2 (artificial neural network method), and sn100pn interactions

Table 2 Difference between experimental and calculated energy levels of ^{102}Sn spectra with χ^2 values. Shell model results are obtained using the interactions: sn100pn, fit1, fit2, pc1, and set2

J^π	Exp-sn100pn (MeV)	Exp-fit1 (MeV)	Exp-fit2 (MeV)	Exp-pc1 (MeV)	Exp-set2 (MeV)
0^+	0	0	0	0	0
2^+	−0.211	−0.044	+0.020	+0.008	−0.074
4^+	−0.160	+0.171	+0.215	+0.095	−0.001
6^+	−0.011	+0.170	+0.017	+0.302	+0.057
χ^2	0.038	0.033	0.027	0.057	0.005

Table 3 Difference between experimental and calculated energy levels of ^{104}Sn spectra with χ^2 values. Shell model results are obtained using the interactions: sn100pn, fit1, fit2, pc1, and set2

Jπ	Exp-sn100pn (MeV)	Exp-fit1 (MeV)	Exp-fit2 (MeV)	Exp-pc1 (MeV)	Exp-set2 (MeV)
0^+	0	0	0	0	0
2^+	−0.234	−0.016	+0.023	+0.010	−0.043
4^+	−0.167	+0.177	+0.187	+0.177	−0.001
6^+	−0.024	+0.149	+0.024	+0.371	+0.009
8^+	−0.183	+0.190	+0.036	+0.415	−0.001
10^+	−0.013	+0.310	+0.037	+0.677	+0.03
χ^2	0.059	0.039	0.021	0.286	0.002

Table 4 Difference between experimental and calculated energy levels of ^{106}Sn spectra with χ^2 values. Shell model results are obtained using the interactions: sn100pn, fit1, fit2, pc1, and set2

J^π	Exp-sn100pn (MeV)	Exp-fit1 (MeV)	Exp-fit2 (MeV)	Exp-pc1 (MeV)	Exp-set2 (MeV)
0^+	0	0	0	0	0
2^+	−0.206	+0.038	+0.095	+0.042	+0.005
4^+	−0.173	+0.127	+0.165	+0.260	−0.029
6^+	−0.097	+0.075	−0.066	+0.380	+0.095
8^+	−0.171	+0.165	−0.013	+0.590	+0.130
10^+	−0.227	+0.051	−0.228	+0.623	+0.105
χ^2	0.067	0.021	0.037	0.345	0.012

Table 5 Difference between experimental and calculated energy levels of ^{103}Sn spectra with χ^2 values. Shell model results are obtained using the interactions: sn100pn, fit1, fit2, pc1, and set2

J^{π}	Exp-sn100pn (MeV)	Exp-fit1 (MeV)	Exp-fit2 (MeV)	Exp-pc1 (MeV)	Exp-set2 (MeV)
$5/2^+$	0	0	0	0	0
$7/2^+$	+0.141	−0.088	−0.077	+0.057	−0.072
$11/2^+$	−0.151	+0.004	+0.013	+0.005	+0.070
$13/2^+$	−0.015	−0.032	−0.049	+0.186	−0.100
χ^2	0.750	0.031	0.004	0.051	0.030

Table 6 Difference between experimental and calculated energy levels of ^{105}Sn spectra with χ^2 values. Shell model results are obtained using the interactions: sn100pn, fit1, fit2, pc1, and set2

J^{π}	Exp-sn100pn (MeV)	Exp-fit1 (MeV)	Exp-fit2 (MeV)	Exp-pc1 (MeV)	Exp-set2 (MeV)
$5/2^+$	0	0	0	0	0
$7/2^+$	+0.061	−0.067	−0.039	+0.002	−0.070
$9/2^+$	−0.200	+0.113	+0.123	+0.067	−0.052
$11/2^+$	−0.057	−0.057	−0.017	+0.161	+0.003
$13/2^+$	−0.150	+0.55	+0.033	+0.233	−0.097
$15/2^+$	+0.055	+0.184	+0.186	+0.413	−0.001
$17/2^+$	−0.064	+0.008	−0.108	+0.246	−0.0315
χ^2	0.070	0.051	0.045	0.195	0.026

set2 interaction is the best to reproduce experimental spectra with small values of χ^2. Additionally, the outcomes for the new interactions fit1 and fit2 demonstrate satisfactory agreement in terms of order of magnitude, with χ^2 values ranging between 0.020 and 0.040.

3.4 Shell Model Calculations

We employed the neutron single-particle energy (SPE) values derived from the two distinct second-order polynomial fits (fit1 and fit2), along with the pc1, sn100pn, and set2 interactions, to conduct nuclear shell model calculations, yielding energy spectra for the isotopes $^{102-107}$Sn. All results are compared to the existing experimental data and with each other.

3.4.1 Even Tin Isotopes: $^{102-106}$Sn

The outcomes of the shell model calculations for the nucleus ^{102}Sn, for which only limited experimental data are accessible, are presented in Fig. 4. It is evident that all interactions accurately replicate the spin and parity of the ground state. For the first excited 2^+ state, it is clear that the result obtained by pc1 interaction is the best among them. Also, the results from the interactions, fit1, fit2, and set2, reproduce this state better than sn100pn. Among them, the closest one to the experimental data is fit2. For the two remaining

Table 7 Difference between experimental and calculated energy levels of ^{107}Sn spectra with χ^2 values. Shell model results are obtained using the interactions: sn100pn, fit1, fit2, pc1, and set2

J^{π}	Exp-sn100pn (MeV)	Exp-fit1 (MeV)	Exp-fit2 (MeV)	Exp-pc1 (MeV)	Exp-set2 (MeV)
$5/2^+$	0	0	0	0	0
$7/2^+$	−0.035	−0.033	−0.007	−0.073	−0.066
$3/2^+$	−0.059	+0.377	+0.528	+0.139	+0.040
$9/2^+$	−0.155	+0.153	+0.178	+0.154	−0.090
$11/2^+$	−0.123	+0.060	+0.083	+0.119	+0.051
$13/2^+$	−0.448	−0.136	−0.152	+0.002	−0.332
$15/2^+$	−0.166	+0.050	+0.077	+0.283	−0.152
$17/2^+$	−0.222	−0.114	−0.234	+0.232	−0.308
χ^2	0.161	0.250	1.638	0.164	0.130

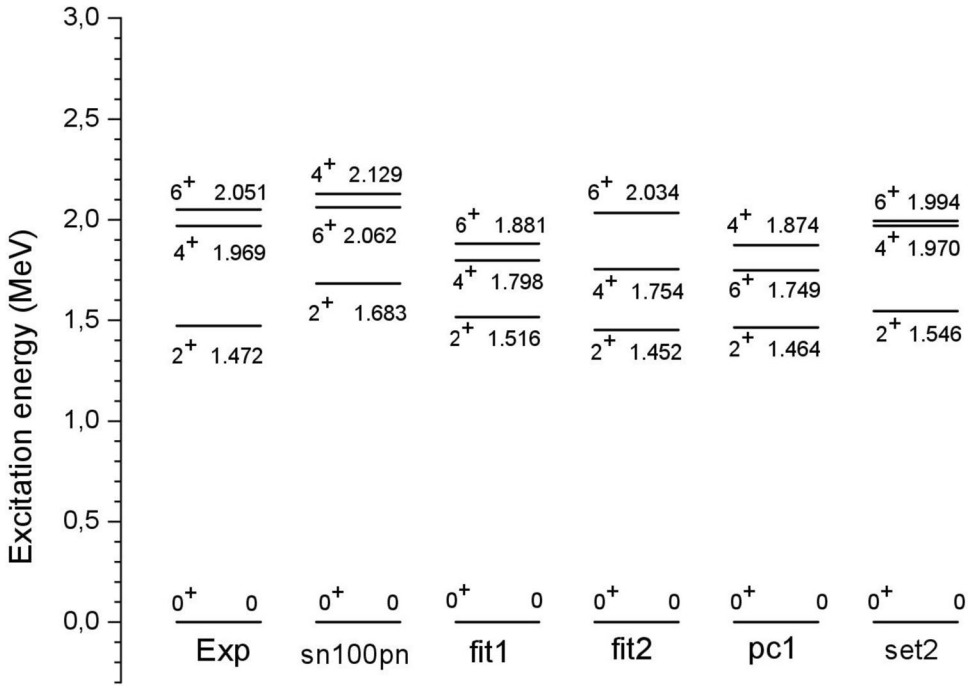

Fig. 4 Shell model calculations for ^{102}Sn nucleus obtained from the different interactions (sn100pn, fit1, fit2, pc1, and set2) in comparison with the experimental data

states in the experimental spectrum, 4^+ and 6^+, pc1 and sn100pn interactions reproduce these levels in inverted order where 6^+ was in its correct position for sn100pn compared to the experiment. In contrast, we obtained these two states in their correct order using the fit1, fit2, and set2 interactions. Fit1 reproduces them lower by 170 keV to the experiment while maintaining the energy difference between them. Fit2 accurately reproduces the 6^+ state, closely matching its exact position, while the 4^+ state is slightly lower by 215 keV compared to the experimental data. Set2 successfully reproduces the 4^+ state in its exact position and the 6^+ state very closely to the experimental value. In general, these two obtained interactions perform better when compared to sn100pn and pc1. Fit2 and set2 demonstrate impressive accuracy, closely replicating the experimental excited states with only small differences in the tens of keV range (except for the 4^+ state in fit2). Table 2 provides a comprehensive list of deviations between the results obtained for the different interactions and the corresponding experimental data.

Shell model calculations performed for the ^{104}Sn isotope using the different interactions are represented in Fig. 5. As it is clearly seen, all the interactions reproduce correctly the spin and parity of all the levels in their correct order. For sn100pn interaction, except 6^+ and 10^+ states, the states are reproduced higher by about 200 keV compared to their corresponding experimental states. For fit1, 2^+ is reproduced in its correct position. All other states are obtained lower than their experimental states by about 150 to 300 keV. On the other hand, for fit2 interaction, besides its reproduction of the correct order of the levels, calculations give results in good agreement with the experimental spectrum for all states to an approximation of few tens of keV, except for 4^+ which is obtained at a level lower by about 180 keV. For pc1 interaction, levels are reproduced in their correct order. With the exception of the 2^+ state, which is accurately reproduced in its position, all the other states appear to be lower in energy compared to their corresponding experimental states. Set2, on the other hand, reproduces all states approximately in their exact positions. Table 3 provides a compilation of the deviations between the results obtained for the various interactions and the corresponding experimental data.

The results of the shell model calculations for ^{106}Sn, using the interactions sn100pn, fit1, fit2, pc1, and set2, are given in Fig. 6 in comparison with the experimental spectrum. All interactions reproduce spins and parities of all states including the ground state in the correct order. For sn100pn interaction, all states are reproduced higher than their corresponding experimental levels. The excited states 2^+ and 10^+ states are higher by more than 200 keV, 4^+ and 8^+ are higher by about 170 keV, and 6^+ is reproduced higher by about 100 keV. For fit1 and fit2 interactions, results are clearly better than those obtained by sn100pn interaction and are in good agreement with the experimental data. Fit1 yields accurate approximations for three out of five states, with deviations less than 100 keV. However, the remaining two states fall short of their corresponding experimental values by approximately 150 keV. In the case of fit2, three states, namely, 2^+, 6^+, and 8^+, are accurately reproduced within an approximation of less than 100 keV. Nevertheless, similar to the findings for isotopes ^{102}Sn and ^{104}Sn, the 4^+ state falls short of the

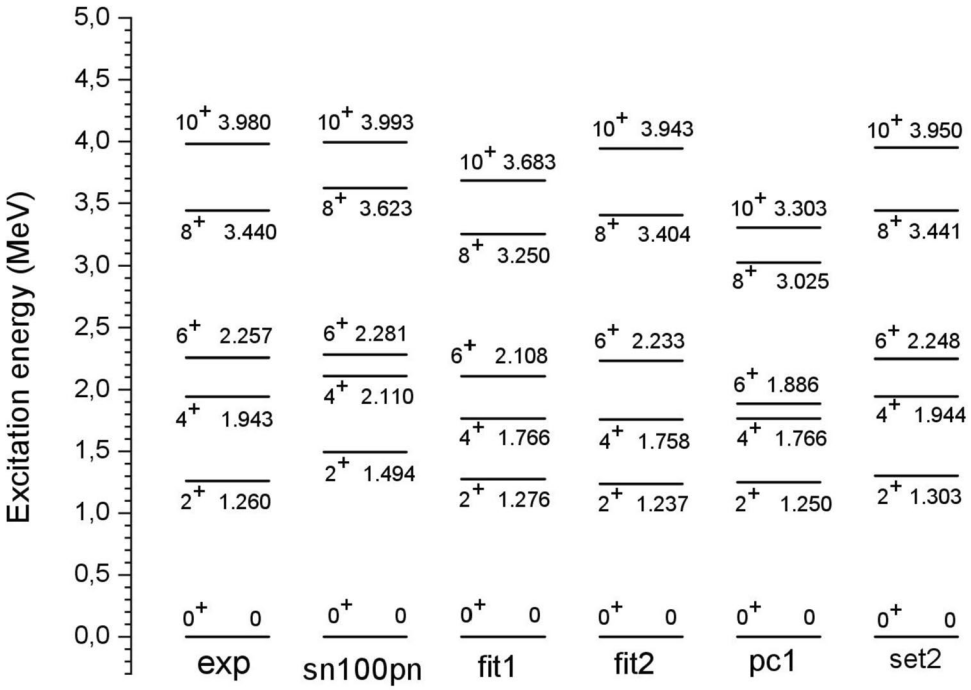

Fig. 5 Shell model calculations for ^{104}Sn nucleus obtained from the different interactions (sn100pn, fit1, fit2, pc1, and set2) in comparison with the experimental data

experimental value by about 160 keV, while the 10^+ state is slightly higher, by approximately 230 keV. When analyzing the results obtained from pc1, it becomes evident that they generally perform worse than those obtained from the other interactions, with all levels calculated at lower values compared to the experimental data. On the other hand, set2 demonstrates good accuracy in reproducing the 2^+ and 4^+ states, while there are differences of approximately 100 keV for the other states when compared to the experimental values. The deviations of the results obtained for different interactions of the experimental data are presented in Table 4.

3.4.2 Odd Tin Isotopes: $^{103-107}$Sn

The results of shell model calculations for ^{103}Sn using the interactions, sn100pn, fit1, fit2, pc1, and set2, compared

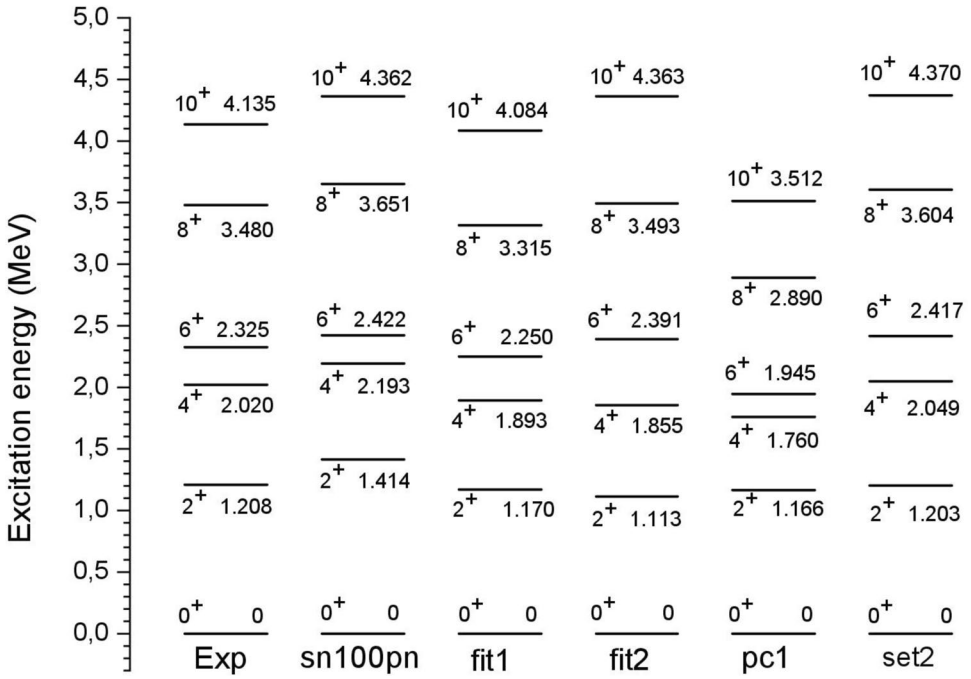

Fig. 6 Shell model calculations for ^{106}Sn nucleus obtained from the different interactions (sn100pn, fit1, fit2, pc1, and set2) in comparison with the experimental data

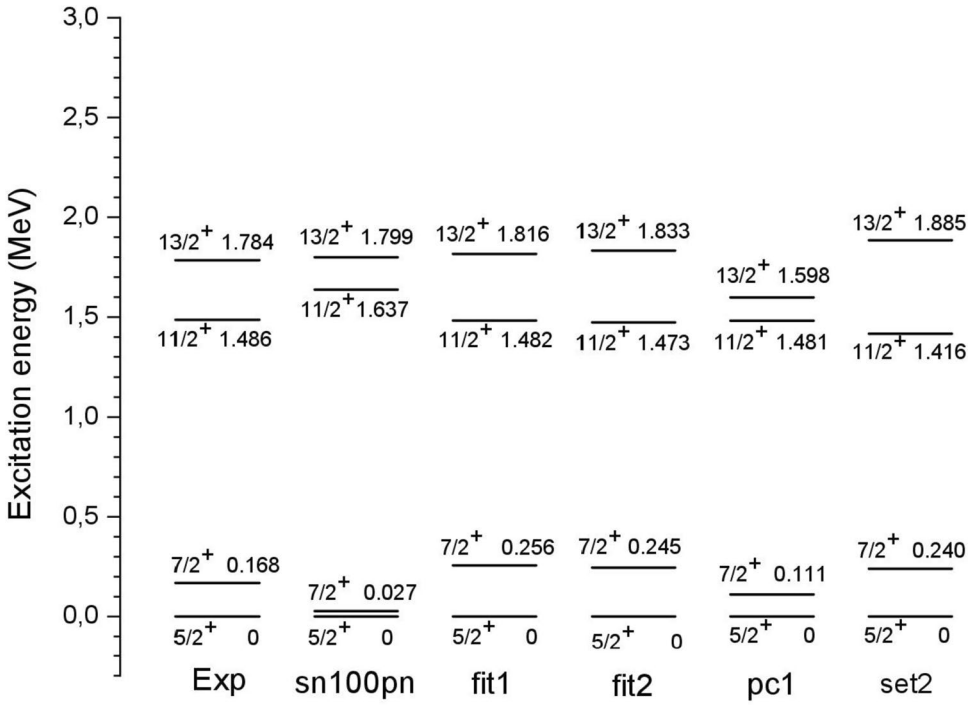

Fig. 7 Shell model calculations for ^{103}Sn nucleus obtained from the different interactions (sn100pn, fit1, fit2, pc1, and set2) in comparison with the experimental data

with its experimental spectrum are given in Fig. 7. It is clear that only four levels exist in its experimental spectrum for this nucleus, which is near the proton drip line. The ground state $5/2^+$ is separated from the first excited state $7/2^+$ by 0.168 MeV. The other two states in the experimental data, $11/2^+$ and $13/2^+$, are determined at slightly higher levels at 1.486 MeV and 1.784 MeV, respectively. By using shell model calculations with sn100pn interaction, all states are reproduced in their correct order. The ground state and the $13/2^+$ state are accurately replicated, closely matching their respective experimental levels. However, the two other states, $7/2^+$ and $11/2^+$, exhibit deviations of approximately 150 keV when compared to their corresponding experimental energy levels. Results obtained by the fit1 and fit2 interactions are much better than the corresponding shell model calculations using the well-known interaction sn100pn. Besides the states are in their correct order, they are all reproduced in a very good agreement compared to the corresponding experimental levels by an approximation of few tens of keV. For the spectrum obtained by using pc1 interaction, it is seen that besides the reproduction of states in their correct order, the first three excited states are in good agreement with the experimental data. Nevertheless, the $13/2^+$ state is reproduced by about 190 keV lower than the known experimental state. Set2 reproduces the states in their correct order with great accuracy. The differences from the experimental values are less than 100 keV. Table 5 lists the deviations of the results for the different interactions from the experimental data.

In Fig. 8, we represent the results of shell model calculations using the sn100pn, fit1, fit2, pc1, and set2 interactions compared to the existing experimental spectrum for ^{105}Sn nucleus. Results obtained by using the sn100pn interaction are generally in fair agreement with the experimental data. The majority of states are reproduced by an approximation of few tens of keV. The two states $9/2^+$ and $13/2^+$ are reproduced higher than their corresponding experimental levels by 200 keV and 150 keV, respectively. The two levels $13/2^+$ and $15/2^+$ are reproduced by this interaction close to each other and in invert order compared to the experimental spectrum for this nucleus. For fit1 results, all states are accurately arranged in their correct order and closely match their corresponding experimental energy levels, with deviations typically within a few tens of keV. However, the $9/2^+$ and $15/2^+$ states are observed at energy levels lower by about 110 keV and 180 keV compared to the experimental values, respectively. In the case of fit2 results, besides the correct order of all states, the $7/2^+$, $11/2^+$, and $13/2^+$ states are well-replicated, displaying good agreement with the experimental spectrum, with deviations typically within a few tens of keV. Similar to fit1, the $9/2^+$ and $15/2^+$ states are observed at levels lower by about 120 keV and 180 keV, respectively, while the $17/2^+$ state is reproduced approximately 100 keV higher in energy compared to the experimental value. For pc1 interaction results, in general, the shell model calculations struggle to accurately reproduce the energy levels in their precise positions, even though the correct order is generally obtained. On the other hand, Set2 performs well by closely

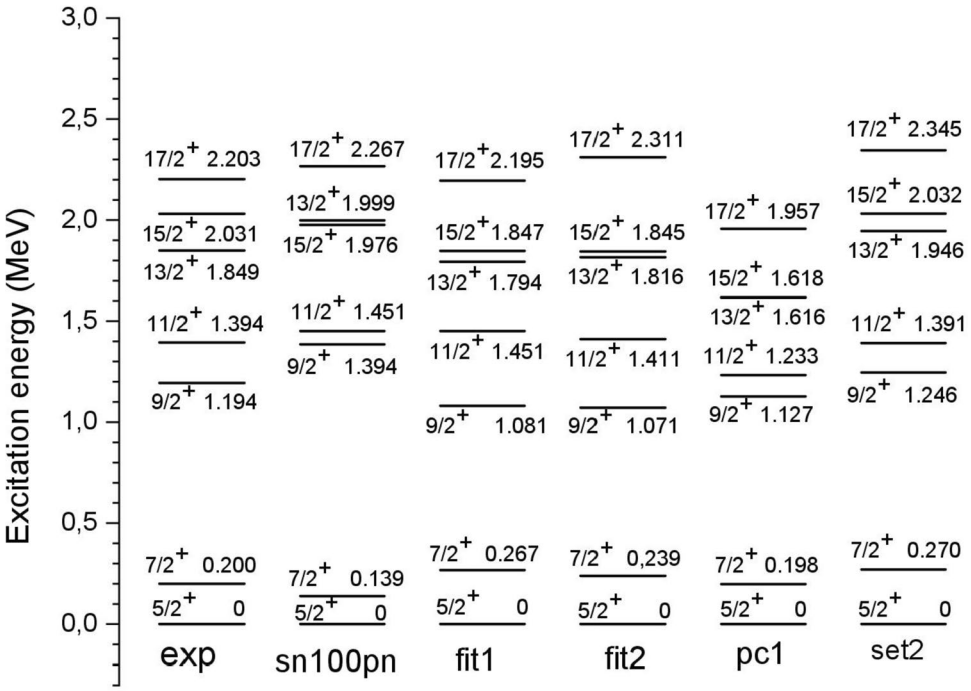

Fig. 8 Shell model calculations for ^{105}Sn nucleus obtained from the different interactions (sn100pn, fit1, fit2, pc1, and set2) in comparison with the experimental data

reproducing the energy levels in their correct positions, with deviations from the experimental data consistently below 100 keV. Overall, the results obtained for the three interactions (fit1, fit2, and set2) exhibit reasonable agreement with the experimental data. Table 6 presents the deviations between the results obtained for various interactions and the experimental data, offering a clear view of these differences.

The results of the shell model calculations for ^{107}Sn using the interactions sn100pn, fit1, fit2, pc1, and set2 are compared with the experimental spectrum in Fig. 9. Using the sn100pn interaction for this nucleus gives results with different accuracies. We can classify levels in three sets. The first set consists of the ground state $5/2^+$ and the two excited states $7/2^+$ and $3/2^+$, respectively. These levels are

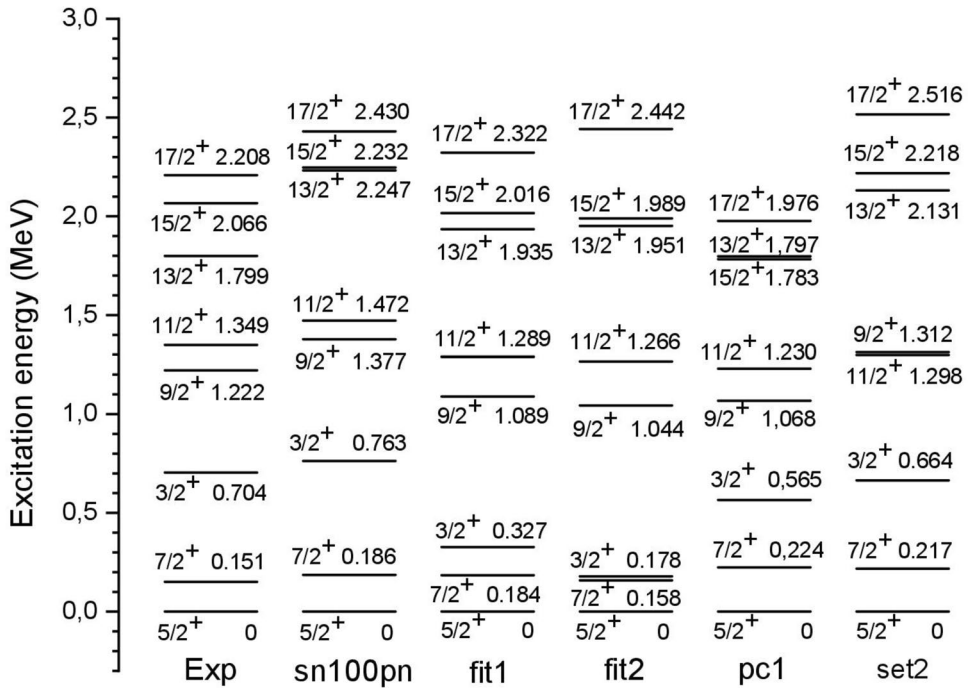

Fig. 9 Shell model calculations for ^{107}Sn nucleus obtained from the different interactions (sn100pn, fit1, fit2, pc1, and set2) in comparison with the experimental data

reproduced in good agreement with the experimental data by differences of about few tens of keV.

The two states, $9/2^+$ and $11/2^+$, comprising the second set, are accurately arranged in the correct order but exhibit slightly higher energy levels, approximately 150 keV and 120 keV higher, respectively, when compared to their corresponding experimental data. The third set of levels encompasses three states: $13/2^+$, $15/2^+$, and $17/2^+$. All levels in this set are reproduced higher with less accuracy going from 160 to 450 keV. In general, for this interaction, only the first three levels including the ground state are reproduced in good agreement with the experiment. In fit1 results, most states, except for the initial $3/2^+$, are accurately reproduced and closely align with their corresponding experimental data. Specifically, the $5/2^+$, $7/2^+$, $11/2^+$, and $15/2^+$ levels exhibit deviations of only a few tens of keV. However, the $9/2^+$, $13/2^+$, and $17/2^+$ levels are replicated with deviations ranging between approximately 110 and 150 keV from their respective experimental levels. Notably, for the $3/2^+$ level, shell model calculations utilizing the fit1 interaction encounter difficulties, as the level is predicted to be lower by approximately 380 keV compared to the corresponding experimental value. For fit2 interaction results, besides the reproduction of the ground state, the four levels, $5/2+$, $7/2^+$, $11/2^+$, and $15/2^+$, are reproduced in good agreement with the experimental spectrum by differences of about few tens of keV. In contrast, shell model calculations using this interaction reproduce three other levels, $9/2^+$, $13/2^+$, and $17/2^+$, with less accuracy by differences from the corresponding experimental values of about 150 to 230 keV. It is clear that this interaction also failed to reproduce the $3/2^+$ level. The difference between fit2 result for this level and the corresponding experimental value is more than 520 keV. In the case of the pc1 interaction, most states, except for the $5/2^+$, $7/2^+$, and $13/2^+$ levels, are obtained at slightly lower energy levels compared to their corresponding experimental values, with differences ranging from 120 to 280 keV. For the set2 interaction, the $5/2^+$, $7/2^+$, $3/2^+$, $9/2^+$, and $11/2^+$ levels closely match their corresponding experimental values, with deviations typically within a few tens of keV. However, the $13/2^+$, $15/2^+$, and $17/2^+$ levels are reproduced at higher energy levels, albeit with less accuracy, with differences ranging from 150 to 330 keV. Overall, for this nucleus, set2 demonstrates the best performance in reproducing the experimental spectrum compared to sn100pn, fit1, fit2, and pc1 interactions. The higher χ^2 values for the fit1 and fit2 interaction results are primarily attributed to the significant differences observed for the first $3/2+$ level. A detailed breakdown of the deviations between the results for different interactions and the corresponding experimental data is provided in Table 7.

4 Conclusions

In this paper, we have used a phenomenological approach based on the experimental data to derive the single-particle states in ^{101}Sn. To accomplish this, we employed two second-order polynomial fits for each set of experimental data pertaining to the states $d_{3/2}$, $s_{1/2}$, and $h_{11/2}$ in light odd Sn isotopes. By extrapolating these curves toward the proton drip line, we were able to derive the energy spectrum of the ^{101}Sn nucleus. Subsequently, we defined SPEs needed in shell model calculations. Shell model calculations of nuclear spectra of light tin isotopes $^{102-107}$Sn have been carried out using the interactions: fit1 and fit2 (obtained by 2nd order polynomial fits), sn100pn (well-known interaction), pc1 (obtained by Hartree–Fock method), and set2 (obtained by ANN method). All results are compared with the experimental spectrum for each nucleus. For even tin $^{102-104}$Sn isotopes, fit2 and set2 interactions are the best compared to results obtained with the other interactions. The results obtained with fit1 and set2 for ^{106}Sn nucleus are in fair agreement with the experiment than the others. For odd isotopes $^{103-107}$Sn, fit2 and set2 interactions generally give better results. The results of this work represent a good support for set2 interaction obtained by ANN method. In the experimental data, the ground state is $5/2^+$ and first excited state is $7/2^+$ in ^{101}Sn nucleus. The fit1, fit2, and set2 interactions correctly preserve the order of these two states within the single-particle energy levels. In contrast, in sn100pn and pc1 interactions, the orders of these levels are inverted. This causes the inverted orders of some states in ^{102}Sn and ^{105}Sn isotopes.

Acknowledgements We acknowledge Prof. Tuncay Bayram, professor at Karadeniz Technical University Trabzon (Turkey), and Prof. Abdelhamid Bouldjedri, professor at Hadj Lakhedar Batna1 University (Algeria) for their help with the Hartree-Fock calculations and discussions.

Data Availability The data that support the findings of this study are available from the corresponding author upon reasonable request.

Declarations

Conflict of Interest The authors declare no competing interests.

References

1. T. Otsuka et al., Novel features of nuclear forces and shell evolution in exotic nuclei. Phys. Rev. Lett. **104**, 012501 (2010)
2. C. Vaman et al., Z=50 shell gap near 100Sn from intermediate-energy Coulomb excitations in even-mass 106–112Sn isotopes. Phys. Rev. Lett. **99**, 162501 (2007)
3. A.V. Afanasjev, D.B. Fossan, G.J. Lane, I. Ragnarsson, Termination of rotational bands: disappearance of quantum many-body collectivity. Phys. Rep. **322**, 1 (1999)

4. A. Holt et al., The structure of neutron deficient Sn isotopes. Nucl. Phys. A **570**, 137 (1994)
5. A. Insolia et al., Microscopic structure of Sn isotopes. Nucl. Phys. A **550**, 34 (1992)
6. Z.H. Sun et al., Effective shell-model interaction for nuclei southeast of ^{100}Sn. Phys. Rev. C **104**, 064310 (2021)
7. A. Yakhelef, A. Bouldjedri, Shell model calculation for Te and Sn isotopes in the vicinity of 100Sn, in The 8th International Conference on Progress in Theoretical Physics(ICPTP 2011), 23–25 October 2011, Constantine, Algeria, edited by N. Mebarki, J. Mimouni, N. Belaloui, and K. Ait Moussa, AIP Conf. Proc. No. 1444 (AIP, New York, 2012), p. 199
8. B.A. Brown, N.J. Stone, J.R. Stone, I.S. Towner, M. Hjorth-Jensen, Magnetic moments of the 2+1 states around 132Sn. Phys. Rev. C **71**, 044317 (2005)
9. A. Hosaka et al., G-matrix effective interaction with the Paris potential. Nucl. Phys. A **444**, 76 (1985)
10. T. Trivedi et al., Shell model description of 102–108Sn isotopes. Int. J. Mod. Phys. E **21**, 1250049 (2012)
11. G.A. Leander et al., Single-particle levels in the doubly magic 132Sn and 100Sn nuclei. Phys. Rev. C **30**, 416 (1984)
12. T. Engeland et al., Large shell model calculations with realistic effective interaction. Phys. Scr. **T56**, 58 (1995)
13. F. Andreozzi, L. Coraggio, A. Covello, A. Gargano, T.T.S. Kuo, Z.B. Li, A. Porrino, Realistic shell-model calculations for neutron deficient Sn isotopes. Phys. Rev. C **54**, 1636 (1996)
14. N. Sandulescu et al., Microscopic description of light Sn isotopes. Nucl. Phys. A **582**, 257 (1995)
15. H. Grawe et al., In-beam spectroscopy of exotic nuclei with OSIRIS and beyond. Prog. Part. Nucl. Phys. **28**, 281 (1992)
16. R. Schubart et al., Shell model structure at ^{100}Sn—the nuclides 98Ag, 103In, and 104–105Sn. Z. Phys. A **352**, 373 (1995)
17. S. Akkoyun, A. Yakhelef, Artificial-intelligence-supported shell-model calculations for light Sn isotopes. Phys. Rev. C **105**, 044309 (2022)
18. M.G. Mayer, On closed shells in nuclei. Phys. Rev. **74**, 235 (1948)
19. I. Talmi, Fifty years of the shell model – the quest for the effective interaction. Adv. Nucl. Phys. **27**, 1 (2003)
20. E. Caurier, G. Martínez-Pinedo, F. Nowack, A. Poves, A.P. Zuker, The shell model as a unified view of nuclear structure. Rev. Mod. Phys. **77**, 427 (2005)
21. B.A. Brown, The nuclear shell model towards the drip lines. Prog. Part. Nucl. Phys. **47**, 517 (2001)
22. B.A. Brown, N.J. Stone, J.R. Stone, I.S. Towner, M. Hjorth-Jensen, Magnetic moments of the 2+ 1 states around 132Sn. Phys. Rev. C **71**, 044317 (2005)
23. C. Lanczos, An iteration method for the solution of the eigenvalue problem of linear differential and integral operators. J. Res. Nat. Bur. Stand. **49**, 255 (1950)
24. Nushell@MSU, B. A. Brown and W. D. M. Rae, MSU-NSCL report (2007)
25. B.A. Brown, W.D.M. Rae, The shell-model code NuShellX@MSU. Nucl. Data Sheets **120**, 115 (2014)
26. BNL Evaluated nuclear structure data file (ENSDF). https://www.nndc.bnl.gov/ensdf/
27. D. Seweryniak et al., Phys. Rev. Lett. **99**, 022504 (2007)
28. I.G. Darby et al., Phys. Rev. Lett. **105**, 162502 (2010)
29. E. Bellotti, C. Broggini, G. DiCarlo, M. Laubenstein, R. Menegazzo, Search for time modulations in the decay constant of ^{40}K and ^{226}Ra at the underground Gran Sasso Laboratory. Phys. Lett. B **780**, 61 (2018)
30. A.W. Steiner, Moving beyond Chi-squared in nuclei and neutron stars. J. Phys. G Nucl. Part Phys. **42**, 034004 (2015)